



# MRI radiomics in the prediction of the volumetric response in meningiomas after gamma knife radiosurgery

Herwin Speckter<sup>1</sup> · Marko Radulovic<sup>2</sup> · Kire Trivodaliev<sup>3</sup> · Velicko Vranes<sup>4</sup> · Johanna Joaquin<sup>1</sup> · Wenceslao Hernandez<sup>1</sup> · Angel Mota<sup>1</sup> · Jose Bido<sup>1</sup> · Giancarlo Hernandez<sup>1</sup> · Diones Rivera<sup>1</sup> · Luis Suazo<sup>1</sup> · Santiago Valenzuela<sup>1</sup> · Peter Stoeter<sup>1</sup>

Received: 8 May 2022 / Accepted: 7 June 2022 / Published online: 17 June 2022

© The Author(s), under exclusive licence to Springer Science+Business Media, LLC, part of Springer Nature 2022

## Abstract

**Purpose** This report presents the first investigation of the radiomics value in predicting the meningioma volumetric response to gamma knife radiosurgery (GKRS).

**Methods** The retrospective study included 93 meningioma patients imaged by three Tesla MRI. Tumor morphology was quantified by calculating 337 shape, first- and second-order radiomic features from MRI obtained before GKRS. Analysis was performed on original 3D MR images and after their laplacian of gaussian (LoG), logarithm and exponential filtering. The prediction performance was evaluated by Pearson correlation, linear regression and ROC analysis, with meningioma volume change per month as the outcome.

**Results** Sixty calculated features significantly correlated with the outcome. The feature selection based on LASSO and multivariate regression started from all available 337 radiomic and 12 non-radiomic features. It selected LoG-sigma-1-0-mm-3D\_firstorder\_InterquartileRange and logarithm\_ngtdm\_Busyness as the predictively most robust and non-redundant features. The radiomic score based on these two features produced an AUC = 0.81. Adding the non-radiomic karnofsky performance status (KPS) to the score has increased the AUC to 0.88. Low values of the radiomic score defined a homogeneous subgroup of 50 patients with consistent absence (0%) of tumor progression.

**Conclusion** This is the first report of a strong association between MRI radiomic features and volumetric meningioma response to radiosurgery. The clinical importance of the early and reliable prediction of meningioma responsiveness to radiosurgery is based on its potential to aid individualized therapy decision making.

**Keywords** Meningioma · Gamma knife · Radiosurgery · Radiomics · Outcome prediction · Machine learning

## Introduction

Stereotactic radiosurgery (SRS) has been used for nearly 40 years in the treatment of meningiomas and there is increasing evidence in support of SRS as primary therapy [1, 2]. Together with improved planning and fractionation regimes, local tumor control rates of up to 99% have been reported after SRS, mainly for small and growth [3, 4]. However, in large volume meningiomas, the control rate may be as low as 84% and even below 70% in atypical and anaplastic types, accompanied by increased radiation-induced toxicity up to 23% [5, 6].

Because of such predictive unreliability, an improved prediction of the individual effectiveness of SRS could help in the treatment planning of individual meningiomas, by supporting an increase in treatment radiation dose or re-evaluation of microsurgery. On the other hand, if a fast and thorough tumor reduction is predicted, a lower dose could be administered to reduce the possible risk of adverse radiation effects (ARE).

Currently used prognostic indicators are clinical symptoms, patient age, general health, neurologic deficit, recurrence after previous treatment, tumor size, localization and delineation against brain tissue and cystic components [7–11]. It was reported that higher meningioma size, fractional anisotropy value [12] and male gender predispose to meningioma progression after treatment with Gamma Knife radiosurgery (GKRS) [13]. In addition, diffusion-weighted

✉ Herwin Speckter  
hspeckter@cedimat.net

Extended author information available on the last page of the article

and diffusion tensor imaging (DWI and DTI) parameters were also investigated as predictors of meningioma type and prognosis after SRS [12, 14–16]. While the first-order texture analysis of MRI data on conventional sequences, fractional anisotropy with other DTI-derived parameter maps and the 3rd eigenvalue of the DTI tensor turned out to correlate best with treatment outcome after SRS, the standard deviation of histograms of T2-weighted images (T2w) best predicted volumetric outcome in conventional sequences [17].

Radiomics is an emerging approach to computational quantification of the tumor morphology for diagnostic, therapeutic, or prognostic decision support [18]. It has been thus far applied to meningioma to predict its grade [19, 20] and the presence of brain invasion [20–24]. The present study was carried out to investigate whether the application of advanced radiomics and feature selection methodology could improve the prediction performance achieved in the previous DTI study [15]. We hypothesized that the currently available tools for the prediction of the volumetric response of meningioma to radiosurgery do not provide sufficient reliability, because they do not fully utilize the morphological heterogeneity of meningioma. The computational radiomic analysis is designed to exploit morphological information that cannot be quantified by visual inspection of MR images. Tumor morphology reflects growth patterns of malignant cells which in turn reflect the sum of molecular interactions within a tumor and thus present a rich source of tumor heterogeneity information.

Based on the pressing need to improve the prediction of meningioma GKRS treatment outcome, the current study is the first attempt to exploit the MRI radiomic analysis to predict the volumetric response to GKRS.

## Methods

This retrospective study was approved by the institutional review board at our center, and informed consent was obtained from all individual participants included in the study. The reporting observes STROBE guidelines for cross-sectional studies that specify consistent reporting of predictive marker research to include all relevant experimental detail.

## Patients

Included were 93 patients between 18.4 and 81.3 years of age (mean = 55.2) with imaging-diagnosed intracranial meningioma treated at our Gamma Knife center. MRI had been performed within 2 months before their radiosurgery, with available follow-up data from at least one MR scan after an

interval of 12 months or longer (range 12.4:77.2 months, mean 35.7; Table 1).

Sixty-nine meningiomas were localized at the cranial base, 15 at the convexity, six at the falx, two at the tentorium and one intraventricularly. We were able to retrieve histology results from 13 to 42 cases in which a preceding operation was documented. Nine of the tumors were characterized as meningothelial and psammomatous meningioma, three as a fibroblastic subtype, one as transitional, all without atypical features. Cases without known histology were assigned as WHO grade I, based on criteria such as homogeneously enhancing, dural tails, no extension through cranial foramina, no substantial peritumoral edema, no significant lobulations. Tumor sizes ranged between 0.48 and 56.7 cm<sup>3</sup> (mean 8.9 cm<sup>3</sup>).

## Gamma Knife treatment

All treatment were performed using a Gamma Knife model 4C (Elekta Instrument AB, Stockholm, Sweden). Details of the Gamma Knife treatment technique were previously described [25], with the exception that at our center, MRI images were acquired up to 2 months before treatment. Performing MRI without the placement of the stereotactic frame can improve image quality, by reducing possible geometric distortions, and permitting higher MRI acquisition acceleration factors, as smaller coils can be selected. On treatment day, after placement of a stereotactic G frame (Elekta AB), MRI sequences were coregistered to the stereotactic contrast-enhanced 3D CT image set.

Depending on tumor size and localization, the margin dose varied from 9.4 to 18 Gy (Table 1). Eighty-one meningiomas were treated in a single session, with margin doses between 11 and 18 Gy (mean 13.7 Gy). According to our institutional protocol, meningioma abutting organs at risk (OAR), particularly the anterior optic pathway (AOP), were treated using hypofractionated radiosurgery (HFSRS). This was the case for 12 meningiomas that were treated with an application of 6 Gy for 3 days or of 5 and 6 Gy for 4 days. Biologically effective dose (BED) is routinely used to compare doses of different dose-fraction regimens, based on the widely accepted linear quadratic (LQ) model, with its acknowledged limitations for high doses [26]. HFSRS doses can be converted to single fraction equivalent doses (SFED) [27], to intuitively compare radiation effects to conventional physical doses of single fraction radiosurgery. Margin SFED of HFSRS treatments varied from 9.4 to 13.5 Gy (mean 11.5 Gy), applying an  $\alpha/\beta$  ratio of 3.76 Gy [28]. Treatments were planned on a Leksell GammaPlan 10.1 workstation (Elekta AB), by optimizing tumor coverage (mean 96.1%), while restricting doses to sensitive structures, such as the AOP, the cochlea, or the brainstem.

**Table 1** Patients, treatment characteristics and treatment results

Patient and treatment characteristics	Value	Range
Number of patients	93	–
Age in years (mean, range)	55.2	(18.4/81.3)
Pre-SRS tumor volume in cm <sup>3</sup> (mean, range)	8.91	(0.48/56.72)
previous RT, SRS	0	–
Single fraction SRS treatments	12	–
KPS before SRS	88.4	60/100
Hypofractionated SRS treatments	81	–
Number of fractions (mean, range)	1.38	(1/4)
Coverage index (mean, range)	96.1%	(56.0%/100%)
Selectivity index (mean, range)	65.9%	(33.0%/99.0%)
Paddick conformity index (mean, range)	63.2%	(32.7%/88.3%)
Margin physical dose in Gy (mean, range)	14.5	(11/24)
Maximum physical dose in Gy (mean, range)	29.0	(22/48)
Margin BED in Gy (mean, range)	62.3	(33.1/104.6)
Margin SFED in Gy (mean, range)	13.4	(9.4/18.0)
Treatment results		
Follow up period in months (mean, range)	35.7	(12.4/77.2)
Complete response	0 [0%]	–
Partial response	13 [14.0%]	–
Minor response	36 [38.8%]	–
Stable disease	37 [39.8%]	–
Progressive disease	7 [7.5%]	–
Absolute volume change in cm <sup>3</sup> (mean, range)	-1.47	(-8.15/22.21)
Relative volume change (mean, range)	-22.5%	(-91.3%/125.4%)
Volume change per month (mean, range)	-0.67%	(-3.46%/5.28%)

SRS stereotactic radiosurgery, RT radiotherapy, GK gamma knife, BED biologically effective dose, SFED single fraction equivalent dose, Gy gray

## MRI

MRI was performed on a 3-Tesla scanner (Achieva; Philips, Eindhoven, Netherlands). Our institutional MRI protocol for pre- and post-Gamma Knife treatment acquisition includes including 3D T1-weighted non-contrast (T1w), contrast-enhanced (CE-T1w), T2w, FLAIR, DWI, DTI, and for selected pathologies sequences as FIESTA, TOF, T2\*w, ASL, QSM. Following parameters were applied for the T1w sequence: 3-dimensional T1 magnetization-prepared rapid acquisition with gradient echo (MP-RAGE), repetition time (TR)/echo time (TE) 6.8/3.2 ms, TI (TFE prepulse) 900 ms, flip angle 8°, measured voxel size 0.6\*0.6\*1.0 mm.

## Postprocessing

In all 93 patients, meningioma volumes were delineated by a neuroradiologist (PS) and neurosurgeons (JB, GH, DR, LS, SV) with respectively 45, 11, 9, 11, 9, 11 years of experience. Tumor volumes were measured from CE-T1w images on the Leksell GammaPlan workstation (version 10.1). All image sets were verified for high image quality. Sequences

with artifacts were excluded. All available sequences for each individual patient were separately uploaded to the QMENTA cloud platform for radiomics analysis.

## Feature extraction

The computational analysis was performed within the boundaries of tumor ROIs by using the open-source Pyradiomics batch extractor [29, 30]. Feature computation was performed on original images and after their transformation by the built-in pre-processing filters: Laplacian of Gaussian (LoG), logarithm and exponential. Six classes of computational image analysis algorithms were employed: first-order statistics, shape descriptors and second-order texture features based on gray-level co-occurrence matrix (GLCM), gray-level size zone matrix (GLSZM), gray-level dependence matrix (GLDM) and neighboring gray-tone difference matrix (NGTDM). Shape-based descriptors were calculated only on unfiltered original images from the label mask, independently of the image's gray values. Radiomics features were extracted from the quality-controlled three-dimensional volumes with z-score normalization but

without re-segmentation. The descriptions of the extracted 337 radiomics features can be found in the PyRadiomics documentation at <https://pyradiomics.readthedocs.io/en/latest/features.html>.

### Sample size calculation

The prospective sample size calculation required 68 patients with 7 positive cases. This calculation was based on the pilot experiment involving 40 patients which delivered the following parameters necessary for sample size calculation:  $\alpha=0.05$ ,  $\beta=0.20$ , and  $AUC=0.79$  (Medcalc 14.8.1; MedCalc Software Ltd., Ostend, Belgium). The actually obtained AUCs for the two calculated radiomic scores were 0.81 (LASSO) and 0.88 (multivariate stepwise regression), with a final sample size of 93 patients.

### Evaluation of predictive performance

Evaluation of the predictive performance for the demographic, MRI, clinicopathological and the radiomic features was approached by the Pearson correlation (Statistica 12, Statsoft, Hamburg, Germany), univariate linear regression (IBM SPSS software package v28, IBM Corporation, Armonk, NY, United States) and receiver operating characteristic (ROC) analysis (IBM SPSS v28), With the meningioma volume change per month as the endpoint. Statistical analyses were based on the continuous values of independent variables and the dependent endpoint variable. The only exception was ROC analysis which can only be calculated by consideration of the categorized dependent variable.

### Model selection

Predictive models were constructed using the features selected by the least absolute shrinkage and selection operator (LASSO) regression (Stata/MP 17, StataCorp, College Station, TX, United States) and stepwise multivariate linear regression (IBM SPSS v28). Both methods were performed by the inclusion of all 284 calculated radiomic features, together with the 12 non-radiomic features listed in Table 2. Of the 284 included radiomic features, LASSO immediately removed 81 based on their collinearity. Features selected by LASSO or stepwise multivariate linear regression were used for the calculation of the Radiomic Scores based on the formula:  $\text{score} = \text{variable1} * \text{coefficient1} + \text{variable2} * \text{coefficient2} + \text{variable3} * \text{coefficient3}$ .

### Validation

The bootstrap technique with 10,000 random resamples of data was applied to adjust the original confidence intervals (95% CIs) and p values, thus correcting for over-optimistic

bias of the univariate linear regression analysis (IBM SPSS v28). Split-sample cross-validation was a validation tool for selecting an optimal penalty coefficient  $\lambda$  within the LASSO regression analysis in Stata/MP 17.

### Follow up

Imaging and clinical follow-up were performed at 6-month intervals for the first 2 years after GKRS, with annual follow-ups thereafter. The volume of meningiomas at the latest imaging follow-up was compared to pre-SRS imaging data and categorized according to RANO criteria for meningiomas [31].

## Results

### Patients' characteristics

The treatment results and characteristics for this patient group are presented in Table 1. After a mean follow-up period of 35.7 months, the control rate was 92.5%. RANO criteria for meningiomas divide response into five types (complete, partial, minor, stable, progressive) based on CE-T1w imaging and meningioma segmentation [31] (Table 1).

The predictive performance of the demographic, MRI and clinicopathological parameters in this patient group is presented in Table 2. The *selectivity index*, *KPS* [32] and *Paddick conformity index* [33] (PCI) reached a significant correlation with the endpoint defined as the change in meningioma volume. The respective Pearson coefficients of 0.257, 0.249 and 0.254 indicated that higher parameter values predicted meningioma progression (Table 2). Unexpectedly, we did not find significant correlations of KPS with either tumor volume pre-SRS ( $p=0.16$ ), nor previous surgery ( $p=0.54$ ), but we found a significant correlation of KPS with age at SRS ( $p \leq 0.01$ ).

### The predictive model for meningioma response to radiosurgery

In total, 337 texture features were extracted from MRIs of 93 meningioma patients for each T1w sequence without and after administration of a contrast agent. Hundred and six features were calculated in original images, 77 in exponentially-, 77 in LoG- and 77 in logarithmically-transformed images. The variability was obtained by 284 features, of which 60 significantly correlated with the meningioma volume change. Eight features with the highest correlation to the outcome are included in Table 2, for T1w sequences without and with contrast, together with their bootstrap-corrected univariate linear regression analysis (Table 2). The odds ratio (OD) designates the effect size of the regression

**Table 2** The predictive performance of the demographic, MRI, clinicopathological and radiomic features

	Pearson coef.	OD (B) <sup>a</sup>	95% CI <sup>b</sup>	P <sup>a</sup>	P bootstrap <sup>b</sup>	F	MSLR coef. <sup>c</sup>	LASSO coef. <sup>d</sup>
Non-radiomic features								
Age at GKRS	0.062	0.006	-0.016/0.028	0.553	0.576	0.36	–	–
Volume before SRS	0.249*	0.026	-0.014/0.083	0.141	0.200	2.19	–	–
Number of fractions	-0.178	-0.266	-0.549/0.015	0.090	0.056	2.97	–	–
SRS total dose to margin	-0.183	-0.101	-0.215/0.007	0.083	0.066	3.16	–	–
BED	0.022	0.002	-0.018/0.23	0.834	0.823	0.04	–	–
SFED	0.020	0.017	-0.142/0.154	0.859	0.828	0.03	–	–
Coverage index	-0.062	-0.020	-0.295/0.008	0.554	0.481	0.35	–	–
Selectivity index	0.257*	0.030	0.005/0.055	0.013	0.016	6.49	–	–
KPS before SRS	0.249*	0.034	0.014/0.057	0.016	0.005	5.99	0.03	–
Paddick conformity index	0.254*	0.032	0.004/0.059	0.014	0.019	6.27	–	–
Radiomic features—without contrast								
LoG-interquartile-range	-0.377	5.8E–5	1.8E–7/0.006	0.000	0.003	14.84	-9.91	-9.92
LoG robust-mean-abs-dev	-0.365	1.7E–10	7.4E–16/6.3E–6	0.000	0.006	13.99	–	–
LoG-mean abs. deviation	-0.343	8.1E–7	1.3E–10/0.0006	0.001	0.002	12.19	–	–
LoG-root mean squared	-0.339	3.9E–5	1.4E–7/0.007	0.001	0.003	11.88	–	–
LoG-variance	-0.337	8.7E–15	7.1E–23/1.1E–7	0.001	0.004	11.66	–	–
LoG-10percentile	0.331	1141	36.9/26903	0.001	0.001	11.20	–	–
Log-ngtdm-busyness	0.322	0.002	0.001/0.003	0.002	0.040	10.58	0.02	0.002
Orig-gldm-lmc1	-0.265	0.070	0.005/0.54	0.013	0.030	6.89	–	–
Radiomic features—with contrast								
Orig_ngtdm_busyness	0.351	0.002	-0.004/0.003	0.001	0.008	12.6	–	–
LoG-gldm-SDLGLE	-0.276	-1011.4	-1813/-181	0.008	0.010	7.40	–	–
Exp_glszm_LargeAreaEmph	0.268	-1.45E–11	-8.1E–12/3.8E–11	0.010	0.210	6.96	–	–
Exp_gldm_DepNonUnif	0.251	6.8E–6	-1.9E–6/1.5E–5	0.016	0.147	6.07	–	–
Exp-gldm_LargeDepEmph	0.244	0.011	0.001/0.022	0.019	0.043	5.68	–	–
Orig-shape_SurfaceVolRatio	-0.242	-4.16	-8.0/0.18	0.020	0.037	5.59	–	–
LoG-glszm_ZoneVariance	0.240	3.68E–9	-2.9E–9/1.1E–8	0.020	0.20	5.50	–	–
Exp-gldm_SmallDepEmph	-0.239	-1416.1	-2682.1/-199.9	0.020	0.030	5.43	–	–

Pearson correlation, linear regression analysis and feature selection by LASSO were all based on the continuous endpoint defined as the percentage of tumor volume change per month

*Exp* exponential, *Orig* original, *Emph* emphasis, *Dep* dependence, *LoG* log-sigma-1-0-mm-3D, *Vol* volume, *SDLGLE* small dependence low gray level emphasis

\*P < 0.05

<sup>a</sup>Univariate linear regression

<sup>b</sup>Univariate linear regression, corrected by bootstrap

<sup>c</sup>Feature selection by the multivariate stepwise linear regression

<sup>d</sup>Feature selection by linear LASSO

(Table 2). Univariate linear regression analysis revealed that texture features overperformed the clinicopathological parameters in association with meningioma volume change (Table 2). It was also obvious that texture features calculated in non-contrast T1w performed better than CE-T1w (Table 2).

It was essential to reduce the number of 60 predictively significant features by selecting those that exhibit the highest predictive robustness and non-redundancy. This was achieved by LASSO and multivariate stepwise

linear regression analyses (Table 3). LASSO regression is a machine learning method that selects covariates and estimates their coefficients by use of the tuning parameter  $\lambda$  in the ten-fold cross-validation. Lasso constantly increases lambda and discards the less important variables when their coefficients shrink to zero (Online resource Fig. 1). Variable selections by LASSO as well as multivariate linear regression were performed by starting from all 284 calculated variables that showed variability. Both methods selected the two identical radiomic



**Table 3** Texture feature selection

LASSO (selected $\lambda = 0.40$ ) <sup>a</sup>	T1 without contrast	
	coefficient (B)	$\lambda$
LoG interquartile range	-9.916	0.53
Log-NGTDM-busyness	0.002	0.46
KPS before GK	–	0.32
Multivariate stepwise linear regression	Coefficient (B)	p value
LoG interquartile range	-8.681	0.000
log-ngtdm-busyness	0.002	0.000
KPS before GKRS	0.028	0.029

KPS karnofsky performance status, GKRS gamma knife radiosurgery,  $\lambda$  a tuning constant used in LASSO variable selection, LASSO least absolute shrinkage and selection operator

Variable selection was performed by LASSO and stepwise multivariate linear regression

<sup>a</sup>Selected  $\lambda = 0.40$ ; based on the lowest predictive error in cross-validation

features in the non-contrast enhanced T1w imaging: LoG Interquartile range and log-NGTDM-Busyness (Online resource Fig. 1, Table 3). Although KPS was not selected by LASSO, it was the first variable just under the selected  $\lambda$  value (Table 3). Neither of the feature selection methods could deliver any features for the CE-T1w sequence. The radiomic scores were calculated by using coefficients and feature values presented in Table 3 and the formula indicated in the Methods section.

The correlation analysis of the two main LASSO-selected predictive features with tumor volume before SRS showed that LoG-Interquartile-Range did not significantly correlate (Pearson coefficient = -0.12;  $p = 0.24$ ), while log-NGTDM-Busyness feature did show a significant positive correlation with tumor volume before SRS (Pearson coefficient = 0.62;  $p = 0.001$ ). This result indicates that larger tumors present more pronounced T1w inhomogeneities, as the inhomogeneity defined by log-NGTDM-Busyness feature is described as the rate of change in greylevel intensities on the very close, neighbouring pixel range.

Unlike LASSO and multivariate regressions, ROC analysis demands a binary outcome. Therefore, the change in meningioma volume was categorized by the three cutpoints, illustrated in Fig. 1A: progressive volume (volumetric change = + 1.5%/month), stable volume (- 0.68%/month) and minor volume (- 1.81%/month). The predictive performance was optimal for the progressive volume cutpoint (+ 1.5%/month) and thereafter declined as the cutpoint was lowered to - 0.68 and - 1.81% (Fig. 1A). The change of meningioma volume in individual patients is presented in Fig. 1a. ROC analysis of radiomic scores is indicated in Fig. 1b.

Figure 2 visually presents the major predictive clue by comparing the T1w images with extreme high and low values of LoG-Interquartile-Range. This feature is of particular

importance because it was selected as the predictively optimal (Tables 2 and 3; Online resource Fig. 1).

Seven cases presented treatment failure with progressive disease after a mean follow-up period of 28.8 months. Pre-SRS tumor volume was on average 11.25 cc [0.95–26.45 cc], all these meningiomas were treated with single fraction SRS with prescription doses of 13.0 Gy on average. Though histology was not available for five cases with progressive disease, pre-SRS histology of the meningioma with largest tumor growth rate (5.3%/m) was described meningothelial, while for the meningioma with third largest growth rate (4.5%/m) pre-SRS histology was obtained as transitional. The LoG-Interquartile-Range value resulted to be on average  $0.1058 \pm 0.0278$  for the seven cases. Malignant transformation was not observed at last imaging follow-up.

## Discussion

Unlike the traditional visual interpretation of morphology seen in medical images, we treated MRI as mineable data by extracting quantitative computational features. This approach gains in importance because increasingly widespread clinical imaging provides an ample source of tumor morphology information with potential predictive value. This report provides the first description of a strong association between imaging features and the volumetric response of meningioma to radiosurgery.

Tumor macroscopic morphological heterogeneity has been increasingly recognized as the source of novel predictive clues for radiotherapy resistance [34, 35]. MRI is commonly used to acquire macroscopic tumor morphology because of its advantages that include specific tissue enhancement, the ability to perform functional, diffusion and perfusion imaging, high contrast and spatial resolution

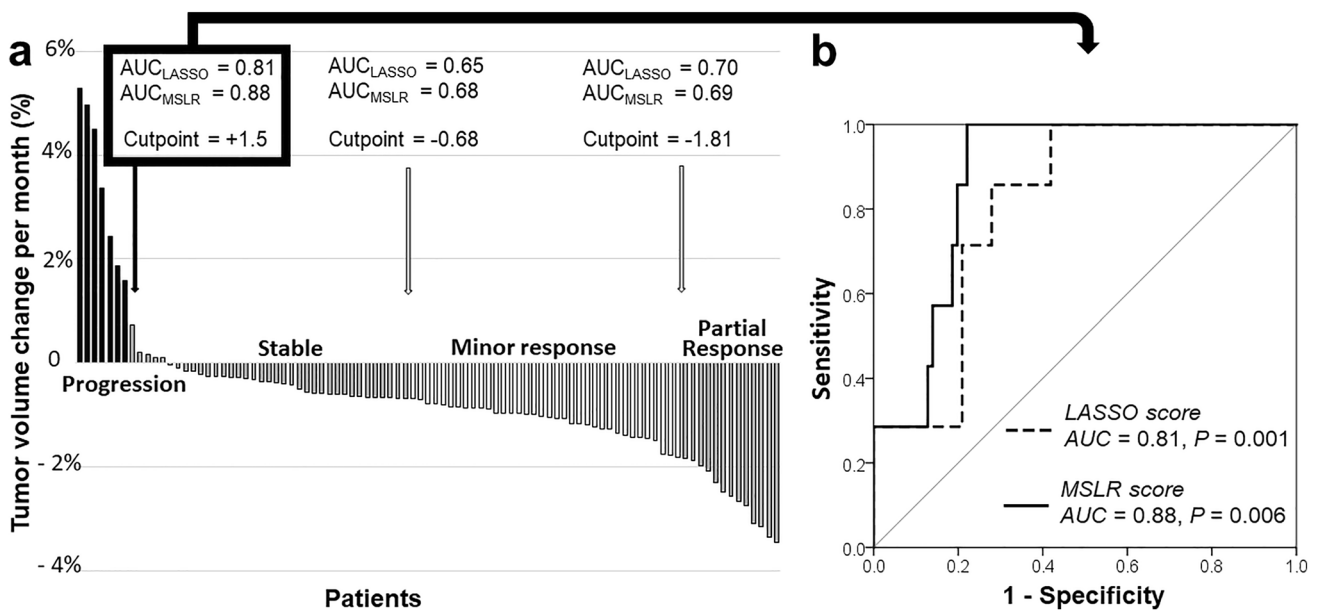


**Fig. 1** Predictive performance of the radiomic scores for different outcomes. **A** Waterfall plot of changes in tumor volume for individual patients. At the time of the last follow-up, seven of 93 meningiomas were characterized as progression (black, left), 37 as stable (gray, middle), 36 as the minor response (white, middle) and 13 as partial response (gray, right). Meningioma volume-outcome was categorized with the indicated three cutpoints. **B** Receiver operating characteristic (ROC) curves for the radiomic scores obtained by linear LASSO

(solid line) and multivariate stepwise linear regression (MSLR, dashed line). The position of predictive scores above the reference line indicates that higher score values predict meningioma progression. Plots reveal discrimination efficiencies of the continuous values of predictive scores calculated against the outcome categorized by the cutoff for meningioma progression defined as +1.5% volume change per month (arrow). *MSLR* multivariate stepwise linear regression, *AUC* area under the curve

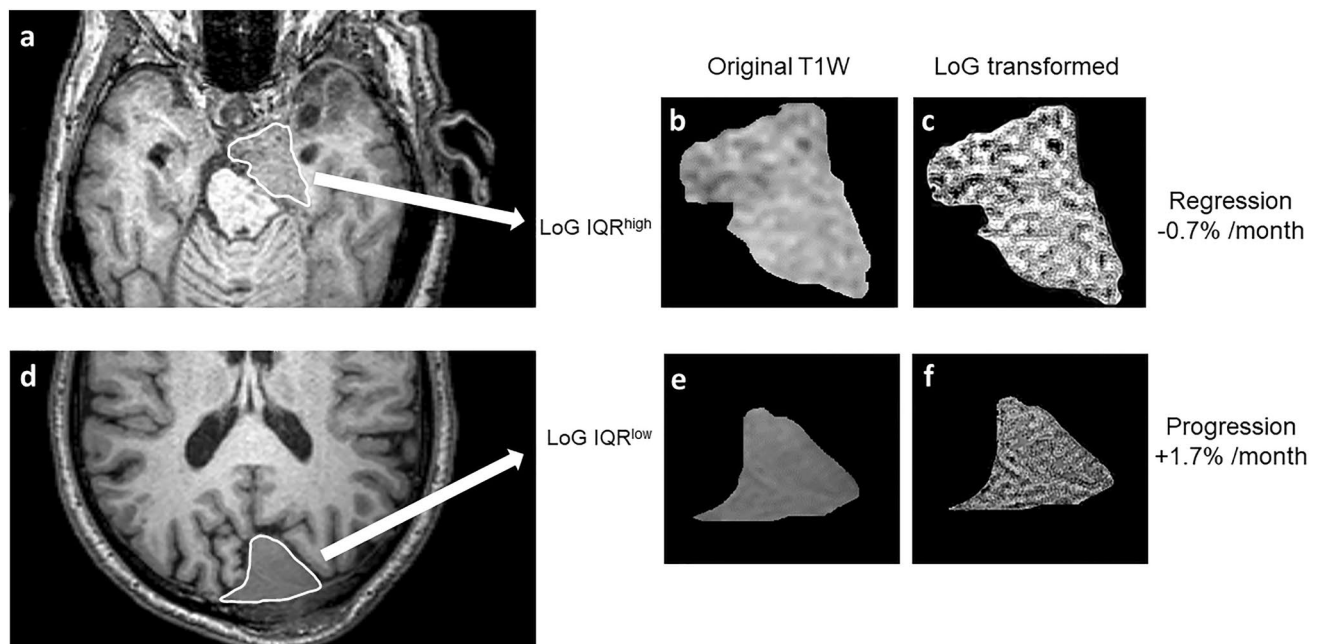


**Fig. 2** Identification of the major morphological predictive clue(s) by visual comparison of MR images with extreme values of LoG-Interquartile-Range as the predictively best-performing feature. **A** Meningioma with volume regression and a high value of LoG-Interquartile-Range. **B** Enlarged ROI of meningioma, shown in **A**. **C** LoG

transformation of the ROI shown in **B**. **D** Meningioma with volume progression and a low value of LoG-Interquartile-Range, **E** Enlarged meningioma ROI from **A**. **F** LoG transformation of the image shown in **B**. *LoG* laplacian of Gaussian, *IQR* interquartile range

[36]. We tried to achieve an exhaustive extraction of the morphological clues in meningioma MRI by calculating the full range of radiomics image-analysis algorithms. Such a comprehensive approach necessitated a reliable feature selection that would reduce the model to a small number of predictively best performing and non-redundant features. The selection results obtained in this study were exceptionally consistent because the two different feature selection methods both selected the same radiomic features for the non-contrast T1w images: LoG Interquartile range and log-NGTDM-Busyness. However, neither of the feature selection methods could identify any sufficiently predictively robust features in the CE-T1w images. This indicated a predictive inferiority of the CE-T1w images.

The LoG-Interquartile-Range is a simple feature describing the difference in pixel intensities between the first and the third image pixel intensity quartiles (25th and 75th percentile). But its interpretation is complicated by the fact that it was calculated on images transformed by the edge detection Laplacian pre-processing filter (LoG), a derivative filter used to highlight areas of rapid change (edges) in images. LoG-Interquartile-Range could be interpreted as a measure of the tumor morphology whereby the larger amount of edges introduced by the LoG pre-processing filter predicted progressive disease. The predictive significance of this feature was previously reported in the single study which exploited T2WI to predict the preoperative T stage in rectal carcinomas [37]. The second selected predictive feature, log-NGTDM-Busyness, was calculated from a neighborhood gray-tone difference matrix (NGTDM) after a logarithmic pre-processing of images. It also reflects the rate of change in greylevel intensities, but on the close range, between the voxel and its 26 immediate neighbors in three dimensions or eight pixels in two dimensions. A high value for busyness defines a complex, ‘busy’ image, with rapid changes of intensity between neighboring pixels and it predicted less favorable volumetric reduction of the meningiomas in the current study. The better-known contrast feature differs from busyness by depending on the dynamic range of pixel intensities, besides the common spatial change rate of pixel intensities. The predictive value of the log-NGTDM-busyness is more established in comparison to the LoG-Interquartile-Range. Log-NGTDM-Busyness was found to discriminate between glioblastoma and primary central nervous system lymphoma [38], it classified PET images of benign and malignant solid pulmonary nodules [39], predicted survival outcomes among lung cancer patients [40] and also predicted tumor aggressiveness [41].

Interestingly, the LoG-Interquartile-Range exerted the opposite predictive association in comparison to the second selected radiomic feature in this study: log-NGTDM-Busyness. The predictive value of both features is presumably derived from their ability to extract tumor texture clues

which alter the tumor volume change rate. Since LoG-Interquartile-Range had a much higher predictive weight within the radiomic score than log-NGTDM-Busyness, it turns out that regions of longer-range rapid intensity changes detected by Laplacian filter are the major predictive clues in meningioma morphology. Our visual investigation of tumor ROI with progression was consistent with the expectation that low LoG-Interquartile-Range values actually reflected higher textural homogeneity. This was consistent with the results of our previous study which calculated the first-order pixel intensity features to find that higher textural homogeneity of T2w images, was associated with tumor progression [17].

The low correlation between treatment plan conformity and volumetric change, expressed by the Coverage Index correlation of  $-0.062$ , indicating a slightly better tumor reduction with higher doses, is probably because most treatment doses were high enough to reach the plateau of the sigmoid curve shoulder of tumor control probability (TCP). Interestingly, the radiation dose did not significantly associate with the outcome, neither was it selected by the feature selection approaches. Control rate for WHO I meningiomas was 92.4% (86 out of 93 cases) at 3 years after SRS was in concordance with literature, progression free survival (PFS) is commonly documented to be in the range 86–99% at 5 years after SRS [42]. The large study led by Santacrose [9], observed a 5-year PFS rate of 95.2%.

Selectivity can be considered as a predictor for normal tissue complication probability (NTCP) and is less frequently considered as an indicator for tumor control. Interestingly, we found that the Selectivity Index reached a significant positive correlation with meningioma volume change, in other words, higher plan selectivity seems to lead to less control. A higher treatment selectivity can be achieved when planning larger or rounder, smooth-edged tumors. While larger tumors are more challenging to control with SRS, additionally, according to our findings, rounder meningiomas appear to have less favorable outcome. Because the Paddick Conformity Index (PCI) is defined as a combination of lesion coverage and selectivity, the significant correlation of selectivity with volume change also reflects in a significant correlation of PCI with volume change.

Advantages of this study include the exceptional consistency of the two used feature selection methods (LASSO and multivariate stepwise regression). This was an indicator of the robustness of our predictive model.

Limitations of this study include the patient group size, although we by far exceeded the sample size requirement, and the patient group was highly homogenized. Furthermore, predictive studies need to establish the generalizability of the obtained results by using internal or external validation. Internal validation is performed within the existing patient group, while external validation uses another



unrelated patient group. The current study performed the internal prognostic validation by the two major approaches: bootstrap bias-correction and cross-validation. Additional validation studies in external groups would be needed to further characterize the prognostic clinical validity of the analysis performed in this study. Furthermore, although the employed computational analysis technique is fully objective, the overall workflow still included residual subjectivity at the level of tumor ROI selection. Lacking pathological characteristics in many cases, the relatively short follow-up period and the retrospective design of the prognostic model were further limitations.

## Conclusion

In conclusion, we report the first strong association between MRI radiomic features and volumetric meningioma response to radiosurgery. Our data indicate that the radiomic texture analysis has the potential to become a useful tool for the identification of novel, independent and predictively more reliable markers for volumetric change, with AUC values reaching 0.88. Pretreatment radiomics analysis can be considered a step towards an automated artificial intelligence-based process to help choose an optimal individualized treatment strategy.

**Supplementary Information** The online version contains supplementary material available at <https://doi.org/10.1007/s11060-022-04063-y>.

**Author contributions** Conception and design: HS and MR. Data collection: HS, JJ, WH, AM, JB, GH, DR, LS, SV, PS. Data analysis and interpretation: All authors. Manuscript writing: HS, MR, PS. All authors reviewed the manuscript.

**Funding** This work was supported by the University Instituto Tecnológico de Santo Domingo (INTEC), Dominican Republic, Grant Number CBA-221024-2020-P-1.

**Data availability** The datasets generated during and analyzed during the current study are available from the corresponding author on reasonable request.

## Declarations

**Conflict of interest** Kire Trivodaliev is employed by QMENTA Inc., Boston, MA, USA. All other authors have nothing to disclose.

## References



- Rogers L, Barani I, Chamberlain M, Kaley TJ, McDermott M, Raizer J, Schiff D, Weber DC, Wen PY, Vogelbaum MA (2015) Meningiomas: knowledge base, treatment outcomes, and uncertainties: a RANO review. *J Neurosurg* 122:4–23. <https://doi.org/10.3171/2014.7.JNS131644>
- Cohen-Inbar O, Lee CC, Sheehan JP (2016) The contemporary role of stereotactic radiosurgery in the treatment of meningiomas. *Neurosurg Clin N Am* 27:215–228. <https://doi.org/10.1016/j.nec.2015.11.006>
- Ius T, Tel A, Minniti G, Somma T, Solari D, Longhi M, De Bonis P, Scerrati A, Caccese M, Barresi V, Fiorentino A, Gorgoglione L, Lombardi G, Robiony M (2021) Advances in multidisciplinary management of skull base meningiomas. *Cancers*. <https://doi.org/10.3390/cancers13112664>
- Sheehan J, Pikis S, Islam AI, Chen CJ, Bunevicius A, Peker S, Samanci Y, Nabeel AM, Reda WA, Tawadros SR, El-Shehaby AMN, Abdelkarim K, Emad RM, Delabar V, Mathieu D, Lee CC, Yang HC, Liscak R, Hanuska J, Alvarez RM, Patel D, Kondziolka D, Moreno NM, Tripathi M, Speckter H, Albert C, Bowden GN, Benveniste RJ, Lunsford LD, Jenkinson MD (2022) An international multicenter matched cohort analysis of incidental meningioma progression during active surveillance or after stereotactic radiosurgery: the IMPASSE study. *Neuro-Oncology* 24:116–124. <https://doi.org/10.1093/neuonc/noab132>
- Fatima N, Meola A, Pollom E, Chaudhary N, Soltys S, Chang SD (2019) Stereotactic radiosurgery in large intracranial meningiomas: a systematic review. *World Neurosurg* 129:269–275. <https://doi.org/10.1016/j.wneu.2019.06.064>
- Helis CA, Hughes RT, Cramer CK, Tatter SB, Laxton AW, Bourland JD, Munley MT, Chan MD (2020) Stereotactic radiosurgery for atypical and anaplastic meningiomas. *World Neurosurg* 144:e53–e61. <https://doi.org/10.1016/j.wneu.2020.07.211>
- DiBiase SJ, Kwok Y, Yovino S, Arena C, Naqvi S, Temple R, Regine WF, Amin P, Guo C, Chin LS (2004) Factors predicting local tumor control after Gamma Knife stereotactic radiosurgery for benign intracranial meningiomas. *Int J Radiat Oncol Biol Phys* 60:1515–1519. <https://doi.org/10.1016/j.ijrobp.2004.05.073>
- Starke RM, Nguyen JH, Rainey J, Williams BJ, Sherman JH, Savage J, Yen CP, Sheehan JP (2011) Gamma Knife surgery of meningiomas located in the posterior fossa: factors predictive of outcome and remission. *J Neurosurg* 114:1399–1409. <https://doi.org/10.3171/2010.11.JNS101193>
- Santacroce A, Walier M, Regis J, Liscak R, Motti E, Lindquist C, Kemeny A, Kitz K, Lippitz B, Martinez Alvarez R, Pedersen PH, Yomo S, Lupidi F, Dominikus K, Blackburn P, Mindermann T, Bundschuh O, van Eck AT, Fimmers R, Horstmann GA (2012) Long-term tumor control of benign intracranial meningiomas after radiosurgery in a series of 4565 patients. *Neurosurgery* 70(1):32–39. <https://doi.org/10.1227/NEU.0b013e31822d408a>
- Sheehan JP, Starke RM, Kano H, Kaufmann AM, Mathieu D, Zeiler FA, West M, Chao ST, Varma G, Chiang VL, Yu JB, McBride HL, Nakaji P, Youssef E, Honea N, Rush S, Kondziolka D, Lee JY, Bailey RL, Kunwar S, Petti P, Lunsford LD (2014) Gamma Knife radiosurgery for sellar and parasellar meningiomas: a multicenter study. *J Neurosurg* 120:1268–1277. <https://doi.org/10.3171/2014.2.JNS13139>
- Mansouri A, Larjani S, Klironomos G, Laperriere N, Cusimano M, Gentili F, Schwartz M, Zadeh G (2015) Predictors of response to Gamma Knife radiosurgery for intracranial meningiomas. *J Neurosurg* 123:1294–1300. <https://doi.org/10.3171/2014.12.JNS141687>
- Cesme DH, Alkan A, Sari L, Yabul F, Temur HO, Aykan ME, Seyithanoglu MH, Hatiboglu MA (2021) Importance of pre-treatment fractional anisotropy value in predicting volumetric response in patients with meningioma treated with Gamma Knife radiosurgery. *Curr Med Imaging* 17:871–877. <https://doi.org/10.2174/2213335608999210128182047>
- O'Connor KP, Algan O, Vesely SK, Palejwala AH, Briggs RG, Conner AK, Cornwell BO, Andrews B, Sughrue ME, Glenn CA (2019) Factors associated with treatment failure and radiosurgery-related edema in WHO grade 1 and 2 meningioma

- patients receiving Gamma Knife radiosurgery. *World Neurosurg* 130:e558–e565. <https://doi.org/10.1016/j.wneu.2019.06.152>
14. Tropine A, Dellani PD, Glaser M, Bohl J, Ploner T, Vucurevic G, Perneczky A, Stoeter P (2007) Differentiation of fibroblastic meningiomas from other benign subtypes using diffusion tensor imaging. *J Magn Reson Imaging* 25:703–708. <https://doi.org/10.1002/jmri.20887>
  15. Speckter H, Bido J, Hernandez G, Mejia DR, Suazo L, Valenzuela S, Perez-Then E, Stoeter P (2016) Prognostic value of diffusion tensor imaging parameters for Gamma Knife radiosurgery in meningiomas. *J Neurosurg* 125:83–88. <https://doi.org/10.3171/2016.7.GKS161455>
  16. Berberat J, Roelcke U, Remonda L, Schwyzer L (2021) Long-term apparent diffusion coefficient value changes in patients undergoing radiosurgical treatment of meningiomas. *Acta Neurochir* 163:89–95. <https://doi.org/10.1007/s00701-020-04567-4>
  17. Speckter H, Bido J, Hernandez G, Rivera D, Suazo L, Valenzuela S, Miches I, Oviedo J, Gonzalez C, Stoeter P (2018) Pretreatment texture analysis of routine MR images and shape analysis of the diffusion tensor for prediction of volumetric response after radiosurgery for meningioma. *J Neurosurg* 129:31–37. <https://doi.org/10.3171/2018.7.GKS181327>
  18. Chang Y, Lafata K, Sun W, Wang C, Chang Z, Kirkpatrick JP, Yin FF (2019) An investigation of machine learning methods in delta-radiomics feature analysis. *PLoS ONE* 14:e0226348. <https://doi.org/10.1371/journal.pone.0226348>
  19. Hu J, Zhao Y, Li M, Liu J, Wang F, Weng Q, Wang X, Cao D (2020) Machine learning-based radiomics analysis in predicting the meningioma grade using multiparametric MRI. *Eur J Radiol* 131:109251. <https://doi.org/10.1016/j.ejrad.2020.109251>
  20. Park YW, Oh J, You SC, Han K, Ahn SS, Choi YS, Chang JH, Kim SH, Lee SK (2019) Radiomics and machine learning may accurately predict the grade and histological subtype in meningiomas using conventional and diffusion tensor imaging. *Eur Radiol* 29:4068–4076. <https://doi.org/10.1007/s00330-018-5830-3>
  21. Kandemirli SG, Chopra S, Priya S, Ward C, Locke T, Soni N, Srivastava S, Jones K, Bathla G (2020) Presurgical detection of brain invasion status in meningiomas based on first-order histogram based texture analysis of contrast enhanced imaging. *Clin Neurol Neurosurg* 198:106205. <https://doi.org/10.1016/j.clineuro.2020.106205>
  22. Hamerla G, Meyer HJ, Schob S, Ginat DT, Altman A, Lim T, Gihl GA, Horvath-Rizea D, Hoffmann KT, Surov A (2019) Comparison of machine learning classifiers for differentiation of grade 1 from higher gradings in meningioma: a multicenter radiomics study. *Magn Reson Imaging* 63:244–249. <https://doi.org/10.1016/j.mri.2019.08.011>
  23. Morin O, Chen WC, Nassiri F, Susko M, Magill ST, Vasudevan HN, Wu A, Vallieres M, Gennatas ED, Valdes G, Pekmezci M, Alcaide-Leon P, Choudhury A, Interian Y, Mortezaei S, Turgutlu K, Bush NAO, Solberg TD, Braunstein SE, Sneed PK, Perry A, Zadeh G, McDermott MW, Villanueva-Meyer JE, Raleigh DR (2019) Integrated models incorporating radiologic and radiomic features predict meningioma grade, local failure, and overall survival. *Neurooncol Adv*. <https://doi.org/10.1093/noonadv/vdz011>
  24. Kalasauskas D, Kronfeld A, Renovanz M, Kurz E, Leukel P, Krenzlin H, Brockmann MA, Sommer CJ, Ringel F, Keric N (2020) Identification of high-risk atypical meningiomas according to semantic and radiomic features. *Cancers*. <https://doi.org/10.3390/cancers12102942>
  25. Patibandla MR, Lee CC, Tata A, Addagada GC, Sheehan JP (2018) Stereotactic radiosurgery for WHO grade I posterior fossa meningiomas: long-term outcomes with volumetric evaluation. *J Neurosurg* 129:1249–1259. <https://doi.org/10.3171/2017.6.JNS17993>
  26. McMahon SJ (2018) The linear quadratic model: usage, interpretation and challenges. *Phys Med Biol* 64:01TR01. <https://doi.org/10.1088/1361-6560/aaf26a>
  27. Speckter H, Santana J, Miches I, Hernandez G, Bido J, Rivera D, Suazo L, Valenzuela S, Garcia J, Stoeter P (2019) Assessment of the alpha/beta ratio of the optic pathway to adjust hypofractionated stereotactic radiosurgery regimens for perioptic lesions. *J Radiat Oncol* 8:279–289. <https://doi.org/10.1007/s13566-019-00398-8>
  28. Vernimmen FJ, Slabbert JP (2010) Assessment of the alpha/beta ratios for arteriovenous malformations, meningiomas, acoustic neuromas, and the optic chiasma. *Int J Radiat Biol* 86:486–498. <https://doi.org/10.3109/09553001003667982>
  29. Fedorov A, Beichel R, Kalpathy-Cramer J, Finet J, Fillion-Robin JC, Pujol S, Bauer C, Jennings D, Fennessy F, Sonka M, Buatti J, Aylward S, Miller JV, Pieper S, Kikinis R (2012) 3D Slicer as an image computing platform for the quantitative imaging network. *Magn Reson Imaging* 30:1323–1341. <https://doi.org/10.1016/j.mri.2012.05.001>
  30. van Griethuysen JJM, Fedorov A, Parmar C, Hosny A, Aucoin N, Narayan V, Beets-Tan RGH, Fillion-Robin JC, Pieper S, Aerts H (2017) Computational radiomics system to decode the radiographic phenotype. *Cancer Res* 77:e104–e107. <https://doi.org/10.1158/0008-5472.CAN-17-0339>
  31. Huang RY, Bi WL, Weller M, Kaley T, Blakeley J, Dunn I, Galanis E, Preusser M, McDermott M, Rogers L, Raizer J, Schiff D, Soffietti R, Tonn JC, Vogelbaum M, Weber D, Reardon DA, Wen PY (2019) Proposed response assessment and endpoints for meningioma clinical trials: report from the response assessment in neuro-oncology working group. *Neuro-Oncology* 21:26–36. <https://doi.org/10.1093/neuonc/nyy137>
  32. Kolakshyapati M, Ikawa F, Abiko M, Mitsuhashi T, Kinoshita Y, Takeda M, Kurisu K (2018) Multivariate risk factor analysis and literature review of postoperative deterioration in karnofsky performance scale score in elderly patients with skull base meningioma. *Neurosurg Focus* 44:E14. <https://doi.org/10.3171/2018.1.FOCUS17730>
  33. Paddick I (2000) A simple scoring ratio to index the conformity of radiosurgical treatment plans: technical note. *J Neurosurg* 93(Suppl 3):219–222. <https://doi.org/10.3171/jns.2000.93.supplement>
  34. O'Connor JPB (2017) Cancer heterogeneity and imaging. *Semin Cell Dev Biol* 64:48–57. <https://doi.org/10.1016/j.semcdb.2016.10.001>
  35. Yang HC, Wu CC, Lee CC, Huang HE, Lee WK, Chung WY, Wu HM, Guo WY, Wu YT, Lu CF (2021) Prediction of pseudoprogression and long-term outcome of vestibular schwannoma after Gamma Knife radiosurgery based on preradiosurgical MR radiomics. *Radiother Oncol* 155:123–130. <https://doi.org/10.1016/j.radonc.2020.10.041>
  36. Wald LL (2019) Ultimate MRI. *J Magn Reson* 306:139–144. <https://doi.org/10.1016/j.jmr.2019.07.016>
  37. You J, Yin J (2021) Performances of whole tumor texture analysis based on MRI: predicting preoperative T stage of rectal carcinomas. *Front Oncol* 11:678441. <https://doi.org/10.3389/fonc.2021.678441>
  38. Xiao DD, Yan PF, Wang YX, Osman MS, Zhao HY (2018) Glioblastoma and primary central nervous system lymphoma: preoperative differentiation by using MRI-based 3D texture analysis. *Clin Neurol Neurosurg* 173:84–90. <https://doi.org/10.1016/j.clineuro.2018.08.004>
  39. Chen S, Harmon S, Perk T, Li X, Chen M, Li Y, Jeraj R (2019) Using neighborhood gray tone difference matrix texture features on dual time point PET/CT images to differentiate malignant from benign FDG-avid solitary pulmonary nodules. *Cancer Imaging* 19:56. <https://doi.org/10.1186/s40644-019-0243-3>

40. Perez-Morales J, Tunali I, Stringfield O, Eschrich SA, Balagurunathan Y, Gillies RJ, Schabath MB (2020) Peritumoral and intratumoral radiomic features predict survival outcomes among patients diagnosed in lung cancer screening. *Sci Rep* 10:10528. <https://doi.org/10.1038/s41598-020-67378-8>
41. Baidya Kayal E, Kandasamy D, Khare K, Bakhshi S, Sharma R, Mehndiratta A (2021) Texture analysis for chemotherapy response evaluation in osteosarcoma using MR imaging. *NMR Biomed* 34:e4426. <https://doi.org/10.1002/nbm.4426>
42. Lee CC, Trifiletti DM, Sahgal A, DeSalles A, Fariselli L, Hayashi M, Levivier M, Ma L, Alvarez RM, Paddick I, Regis J, Ryu S, Slotman B, Sheehan J (2018) Stereotactic radiosurgery for benign (World Health Organization Grade I) cavernous sinus meningiomas-international stereotactic radiosurgery society (ISRS) practice guideline: a systematic review. *Neurosurgery* 83:1128–1142. <https://doi.org/10.1093/neuros/nyy009>

**Publisher's Note** Springer Nature remains neutral with regard to jurisdictional claims in published maps and institutional affiliations.

## Authors and Affiliations

Herwin Speckter<sup>1</sup>  · Marko Radulovic<sup>2</sup>  · Kire Trivodaliev<sup>3</sup> · Velicko Vranes<sup>4</sup> · Johanna Joaquin<sup>1</sup> · Wenceslao Hernandez<sup>1</sup> · Angel Mota<sup>1</sup> · Jose Bido<sup>1</sup> · Giancarlo Hernandez<sup>1</sup> · Diones Rivera<sup>1</sup> · Luis Suazo<sup>1</sup> · Santiago Valenzuela<sup>1</sup> · Peter Stoeter<sup>1</sup>

Marko Radulovic  
marko@radulovic.net

Kire Trivodaliev  
kire.trivodaliev@qmenta.com

Velicko Vranes  
vellioni@yahoo.com

Johanna Joaquin  
yoany26@hotmail.com

Wenceslao Hernandez  
whernandez4md@gmail.com

Angel Mota  
angelmota98@gmail.com

Jose Bido  
Josebido1@yahoo.com

Giancarlo Hernandez  
neurogh@hotmail.com

Diones Rivera  
dionesrivera@gmail.com

Luis Suazo  
lsuazo@cedimat.net

Santiago Valenzuela  
stgo.sosa@gmail.com

Peter Stoeter  
Peter.stoeter@gmx.de

<sup>1</sup> Centro Gamma Knife Dominicano and Department of Radiology, CEDIMAT, Plaza de la Salud, Santo Domingo, Dominican Republic

<sup>2</sup> Department of Experimental Oncology, Institute for Oncology & Radiology of Serbia, Pasterova 14, 11000 Belgrade, Serbia

<sup>3</sup> QMENTA Inc., Boston, MA, USA

<sup>4</sup> Instituto Tecnológico de Santo Domingo (INTEC), Santo Domingo, Dominican Republic